Bioresource Technology 146 (2013) 152–160

Contents lists available at ScienceDirect

Bioresource Technology

journal homepage: www.elsevier.com/locate/biortech

Biomass torrefaction characteristics in inert and oxidative atmospheres at various superficial velocities

Wei-Hsin Chen [a,*], Ke-Miao Lu [b], Shih-Hsien Liu [c], Chi-Ming Tsai [c], Wen-Jhy Lee [b,*], Ta-Chang Lin [b]

[a] Department of Aeronautics and Astronautics, National Cheng Kung University, Tainan 701, Taiwan, ROC
[b] Department of Environmental Engineering, National Cheng Kung University, Tainan 701, Taiwan, ROC
[c] Iron and Steel Research and Development Department, China Steel Corporation, Kaohsiung 812, Taiwan, ROC

HIGHLIGHTS

- Non-oxidative and oxidative torrefaction of biomass are studied.
- The superficial velocity or volumetric flow rate of carrier gas is altered.
- Thermal degradation of biomass in N_2 is controlled by internal heat and mass transfer.
- Torrefaction reaction of biomass in air is dominated by surface oxidation.
- There exists an upper limit of air superficial velocity in the decrement of solid yield.

GRAPHICAL ABSTRACT

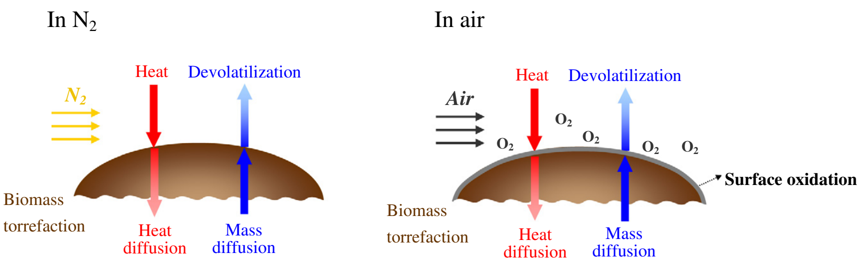

ARTICLE INFO

Article history:
Received 10 May 2013
Received in revised form 13 July 2013
Accepted 15 July 2013
Available online 21 July 2013

Keywords:
Non-oxidative and oxidative torrefaction
Fibrous and ligneous biomass
Superficial velocity
Heat and mass transfer
Energy yield

ABSTRACT

The reaction characteristics of four biomass materials (i.e. oil palm fiber, coconut fiber, eucalyptus, and *Cryptomeria japonica*) with non-oxidative and oxidative torrefaction at various superficial velocities are investigated where nitrogen and air are used as carrier gases. Three torrefaction temperatures of 250, 300, and 350 °C are considered. At a given temperature, the solid yield of biomass is not affected by N_2 superficial velocity, revealing that the thermal degradation is controlled by heat and mass transfer in biomass. Increasing air superficial velocity decreases the solid yield, especially in oil palm fiber and coconut fiber, implying that the torrefaction reaction of biomass is dominated by surface oxidation. There exists an upper limit of air superficial velocity in the decrement of solid yield, suggesting that beyond this limit the thermal degradation of biomass is no longer governed by surface oxidation, but rather is controlled by internal mass transport.

© 2013 Elsevier Ltd. All rights reserved.

1. Introduction

Biomass is considered as an important renewable fuel. However, its energy density is lower than fossil fuel; this leads to the low utilization efficiency when biomass is directly consumed as a fuel. To overcome this disadvantage, the energy density of biomass can be improved via physical or thermal processes, such as volume reduction (compression), pelletization, and torrefaction (Chiang et al., 2012). Torrefaction is a thermal pretreatment process for biomass heated at temperatures of 200–300 °C in an inert atmosphere for several minutes to several hours. The properties of biomass are improved following torrefaction and this increases the energy density of biomass (Chew and Doshi, 2011; Chen et al., 2011a,b; Uemura et al., 2011; Peng et al., 2012; Tapasvi et al., 2012; Tran et al., 2013). Li et al. (2012a) reported that torrefaction was able to give a high substitution ratio of biomass in a co-firing process, and the net emissions of CO_2 and NO_x were obviously reduced by increasing the substitution ratio in the co-firing system. When torrefied biomass was blended with coal to be pyrolyzed, Lu et al. (2012a) discovered that the interaction or synergistic effect between the two different materials was slight.

---

* Corresponding authors. Tel.: +886 6 2757575x63600; fax: +886 6 2389940 (W.-H. Chen). Tel.: +886 6 2757575x65831; fax: +886 6 2752790 (W.-J. Lee).

E-mail addresses: weihsinchen@gmail.com (W.-H. Chen), wjlee@mail.ncku.edu.tw (W.-J. Lee).

0960-8524/$ - see front matter © 2013 Elsevier Ltd. All rights reserved.
http://dx.doi.org/10.1016/j.biortech.2013.07.064

In recent years the substitution of biomass for fossil fuels has become increasingly prevalent. Because of this, more and more research has been performed on torrefaction since 2005, and many studies have been published after 2010. The studies of torrefaction can roughly be cataloged into two topics; one is the kinetics of torrefaction and the other is the properties of torrefied biomass. In respect of torrefaction kinetics, Prins et al. (2006) stated that the kinetics of torrefaction reactions could be described by a two-step mechanism; the first step involved hemicellulose decomposition and the second step involved cellulose decomposition. Chen and Kuo (2011) investigated the torrefaction kinetics of hemicellulose, cellulose, and lignin at 220–300 °C. They found that hemicellulose and cellulose were sensitive to torrefaction at temperatures higher than 250 and 275 °C, respectively. With regard to lignin, its thermal degradation was relatively insensitive to torrefaction within the investigated temperature range. A number of studies have analyzed the effects of torrefaction temperature and duration on the energy yield and properties of biomass. In general, the impact of torrefaction temperature on biomass was greater than the impact of duration (Chen et al., 2011a, 2012a; Tapasvi et al., 2012; Duncan et al., 2013).

Aside from convectional torrefaction, a variety of torrefaction methods have also been developed to upgrade biomass. They include wet torrefaction (Yan et al., 2009) or torrefaction with dilute acid solutions (Lynam et al., 2011), microwave torrefaction (Huang et al., 2012), the combination of wet torrefaction and microwave-assisted heating (Chen et al., 2011c, 2012b), biomass torrefied in a fluidized bed reactor (Li et al., 2012b,c; Rousset et al., 2012a), and biomass torrefaction in elevated pressure environments (Wannapeera and Worasuwannarak, 2012). The properties of torrefied biomass are more uniform and the thermal efficiency is enhanced, regardless of what kind of torrefaction method is utilized. Conventional torrefaction is carried out in a nitrogen atmosphere, which leads to a higher operating cost, stemming from the requirement of N_2 separation from air. Oxidative torrefaction is another special torrefaction process in which biomass is torrefied in an oxidative environment. Air is usually employed as the carrier gas so as to reduce the consumption of N_2 and operating costs. Wang et al. (2013) found that the properties of torrefied sawdust and its pellets in oxidative environments, such as density, energy consumption for pelletization, higher heating value, and energy yield, were similar to those in inert atmospheres. They also concluded that using oxygen laden combustion flue gases as carrier gases for the torrefaction of biomass were feasible.

The thermal degradation characteristics of biomass pyrolyzed in oxidative environments have been examined by a number of researchers through the thermogravimetric analysis. Fang et al. (2006) and Chouchene et al. (2010) indicated that an increase in oxygen concentration resulted in a lower thermal degradation temperature and a higher decomposition rate. Chouchene et al. (2010) and Ghetti et al. (1996) pointed out that the beginning of thermal degradation temperature for biomass in air was lower and its decomposition rate was faster when compared to biomass in nitrogen. Devolatilization is an important mechanism for the thermal degradation of biomass in an inert atmosphere. On the other hand, biomass oxidation is another remarkable mechanism when the material is thermally degraded in an oxidative environment (Fang et al., 2006; Chouchene et al., 2010; Munir et al., 2009; Wongsiriamnuay and Tippayawong, 2010). For example, Uemura et al. (2013) described the oxidative torrefaction of biomass as proceeding in two successive steps; the first was ordinary torrefaction and the other was biomass oxidation. With oxidative torrefaction, an increase in reaction temperature or oxygen concentration decreases the solid yield of biomass (Lu et al., 2012b; Rousset et al., 2012b; Uemura et al., 2013), and normally the impact of temperature on biomass prevails over the oxygen concentration. The heat and mass transfer as well as oxidation reaction around biomass in both inert and oxidative environment are sketched in Fig. 1.

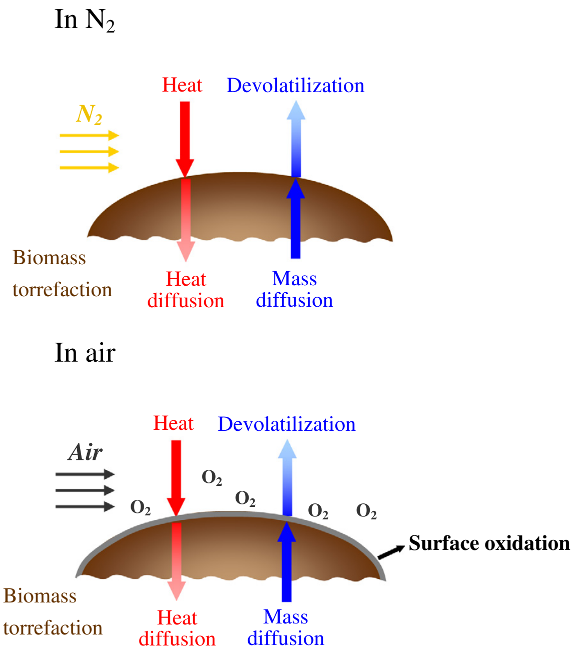

Fig. 1. A schematic of heat and mass transfer as well as oxidative reaction around biomass.

In oxidative torrefaction, the influences of torrefaction temperature and oxygen concentration on the performance of biomass torrefaction have been studied (Rousset et al., 2012b; Uemura et al., 2013). However, the effect of the superficial velocity or the flow rate of carrier gas on biomass torrefaction has not been explored yet. In addition to oxygen concentration, the superficial velocity of the carrier gas is also consequential in terms of operating costs. The objectives of this study are to investigate the impact of the superficial velocity or the flow rate of carrier gas on the properties of biomass and the performance of oxidative torrefaction. The torrefaction temperature is normally controlled below 300 °C. To give a wider insight into the operation of oxidative torrefaction, three torrefaction temperatures of 250, 300, and 350 °C will be taken into consideration. Detailed reaction mechanisms for non-oxidative and oxidative torrefaction will be addressed.

2. Materials and methods

2.1. Material

The present study investigates four types of biomass; they are oil palm fiber (OPF), coconut fiber (CF), eucalyptus (EU), and *Cryptomeria japonica* (CJ). OPF and CF pertain to fibrous biomass, whereas EU and CJ belong to ligneous biomass. The properties of the four untreated materials (i.e. material size, fiber, proximate, elemental, and calorific analyses) are listed in Table 1.

2.2. Experimental setup

The system was made up of a gas supply unit, a reactor, a cooling unit, and a gas treatment unit. Two mass flow controllers (Alicat Scientific) were used to individually control the superficial velocity or the flow rates of N_2 and air (carrier gas) in the gas supply unit. The mass flow controllers were calibrated by a flow

Table 1
A list of the properties of four tested biomass materials.

Biomass	Oil palm fiber	Coconut fiber	Eucalyptus	*Cryptomeria japonica*
Material size (mm)	Length < 30	Length < 30	15 × 10 × 5	15 × 10 × 5
Fiber analysis (wt%, db[a]*)*				
Hemicellulose	34.00	12.50	15.35	16.01
Cellulose	26.78	47.10	48.36	43.60
Lignin	16.08	31.35	21.26	32.20
Other	23.14	9.05	15.03	8.19
Proximate analysis (wt%, db)				
Volatile matter (VM)	72.46	75.64	81.07	80.82
Fixed carbon (FC)	20.51	23.72	18.93	19.18
Ash	7.03	0.64	0.00	0.00
Elemental analysis (wt%, daf[b]*)*				
C	51.94	51.77	50.77	51.73
H	4.75	4.43	5.13	5.30
O[c]	40.88	42.87	44.10	42.80
N	2.43	0.93	0.00	0.17
HHV (MJ kg^{-1}, db)	17.13	18.25	18.38	18.59

[a] Dry basis.
[b] Dry-ash-free.
[c] By difference, O (wt%) = 100 − C − H − N.

calibrator (mini-Buck Calibrator M-30) to ensure the precision of the controllers. The reactor comprised a heater and a cylindrical chamber. The heater was utilized to elevate and maintain the reaction temperature and it was controlled by a heater controller. The height and the diameter of the cylindrical chamber in which the biomass samples were tested, were 440 and 125 mm, respectively. The cooling unit consisted of a vessel, a water cooler, and a nitrogen supplier to cool the torrefied samples. Nitrogen was blown into the vessel and the vessel was enveloped by a water jacket. Two conical flasks in series were employed in the gas treatment unit.

2.3. Experimental procedure

OPF and CF were trimmed and meshed to lengths of less than 30 mm where needle-shaped materials were obtained. EU and CJ were cut into blocks with the dimensions of 15 × 10 × 5 mm. The samples were dried in an oven at 105 °C until their constant mass was attained. The moisture content was measured by means of a moisture analyzer (Ohaus MB45). The weights of fibrous biomass and ligneous biomass were fixed at 10 g (±5%) and 20 g (±5%), respectively, as a consequence of different appearances and densities. When biomass was torrefied, the duration was fixed at 1 h. The torrefied biomass was placed in the vessel in which nitrogen at a flow rate of 1000 mL min^{-1} (25 °C) was used to directly cool the sample to room temperature. At the same time, the cooling water at a flow rate of 1000 mL min^{-1} (10 °C) was used to cool the vessel. The cooled solid residues were collected for subsequent analyses. After the carrier gas left the reactor, it was washed by water in the two conical flaks to remove tars and clean the exhaust gas.

2.4. Sample analysis

The fiber contents (hemicellulose, cellulose, and lignin) in biomass were analyzed through the measurements of neutral detergent fiber, acid detergent fiber, and ash (Chen et al., 2010). The proximate analysis was performed in accordance with the standard procedure of the American Society for Testing and Materials (ASTM E870-82). The elemental analysis was carried out by use of an elemental analyzer (Vario EL III). The higher heating values (HHVs) of samples were detected by a bomb calorimeter (IKA C2000 Basic).

To ascertain the quality of the experiment and sample analysis, the entire experimental system was leak tested prior to performing experiments. The torrefaction experiment at any given condition and the sample analysis were carried out more than three times. The relative error of the data was less than 5% and the data discussed below were the average results.

3. Results and discussion

3.1. Effect of superficial velocity

Fig. 2a displays the profile of the solid yield of OPF where the biomass is torrefied in a N_2 atmosphere at 300 °C with N_2 superficial velocities between 0.82 and 8.15 cm min^{-1}. The superficial velocity is defined as the volumetric flow rate of carrier gas divided by the cross-sectional area of the cylindrical chamber (Saravanakumar et al., 2007). Accordingly, the N_2 superficial velocities between

(a) N_2 atmosphere

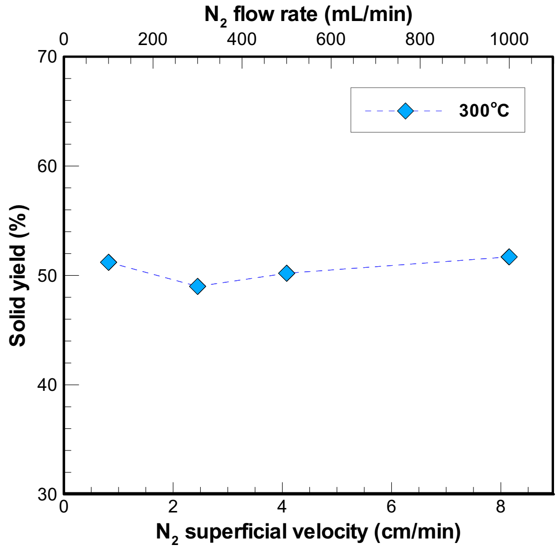

(b) Air atmosphere

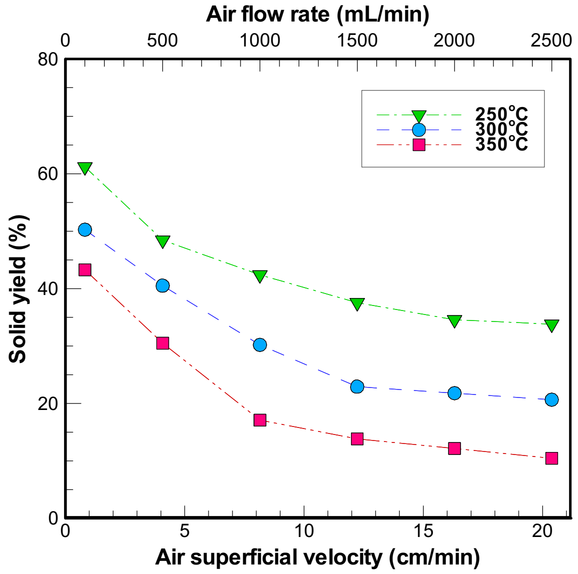

Fig. 2. The profiles of the solid yield of torrefied OPF at various superficial velocities and flow rates of (a) nitrogen and (b) air.

0.82 and 8.15 cm min^{-1} correspond to the N_2 flow rates between 100 and 1000 mL min^{-1}. It can be seen that the solid yield, which is defined as the weight ratio of torrefied biomass and raw biomass and expressed in %, is around 50.5% (±1.2%) and the value is almost invariant when the superficial velocity is altered. Physically, when the devolatilization process occurs along the biomass surface, the liberated volatile matter will be delivered by the carrier gas. The fact that the altered N_2 superficial velocity plays no role in changing the solid yield of OPF means that the performance of torrefaction is controlled by heat and mass transfer in biomass rather than on biomass surface. The profiles of the solid yield of OPF at various torrefaction temperatures and air superficial velocities are displayed in Fig. 2b. Unlike OPF in the N_2 atmosphere, increasing air superficial velocity diminishes the solid yield of OPF, regardless of the torrefaction temperature. This is due to more oxidant supplied for the oxidation of OPF (Uemura et al., 2013). It follows that the oxidative torrefaction of OPF is dominated by surface oxidation. It is not surprising that an increase in torrefaction temperature lowers the solid yield, as a consequence of intensified oxidation at a higher temperature. It is noteworthy that the solid yield is insensitive to the air superficial velocity when it is higher than 12.23 cm min^{-1}. Hence this velocity can be thought of as the upper limit of supplied air for the oxidative torrefaction of OPF in the chamber. From the operating point of view, once the air superficial velocity is higher than this limit, the air supply will be inefficient. This means that the thermal degradation is not governed by surface oxidation. Instead, the reaction may be controlled by internal mass transport.

3.2. Proximate analysis and solid yield

Seeing that the superficial velocity of 12.23 cm min^{-1} can be considered as the upper limit for the supply of air, five cases at different air superficial velocities are studied for comparison. In Case 1, N_2 serves as the carrier gas whose superficial velocity is 8.15 cm min^{-1} (i.e. air flow rate = 1000 mL min^{-1}) and no air is fed. In Cases 2–5, air is adopted as the carrier gas. For Cases 2, 3, 4, and 5, air superficial velocities are 0.82, 4.08, 8.15, and 12.23 cm min^{-1}, respectively, corresponding to the air flow rates

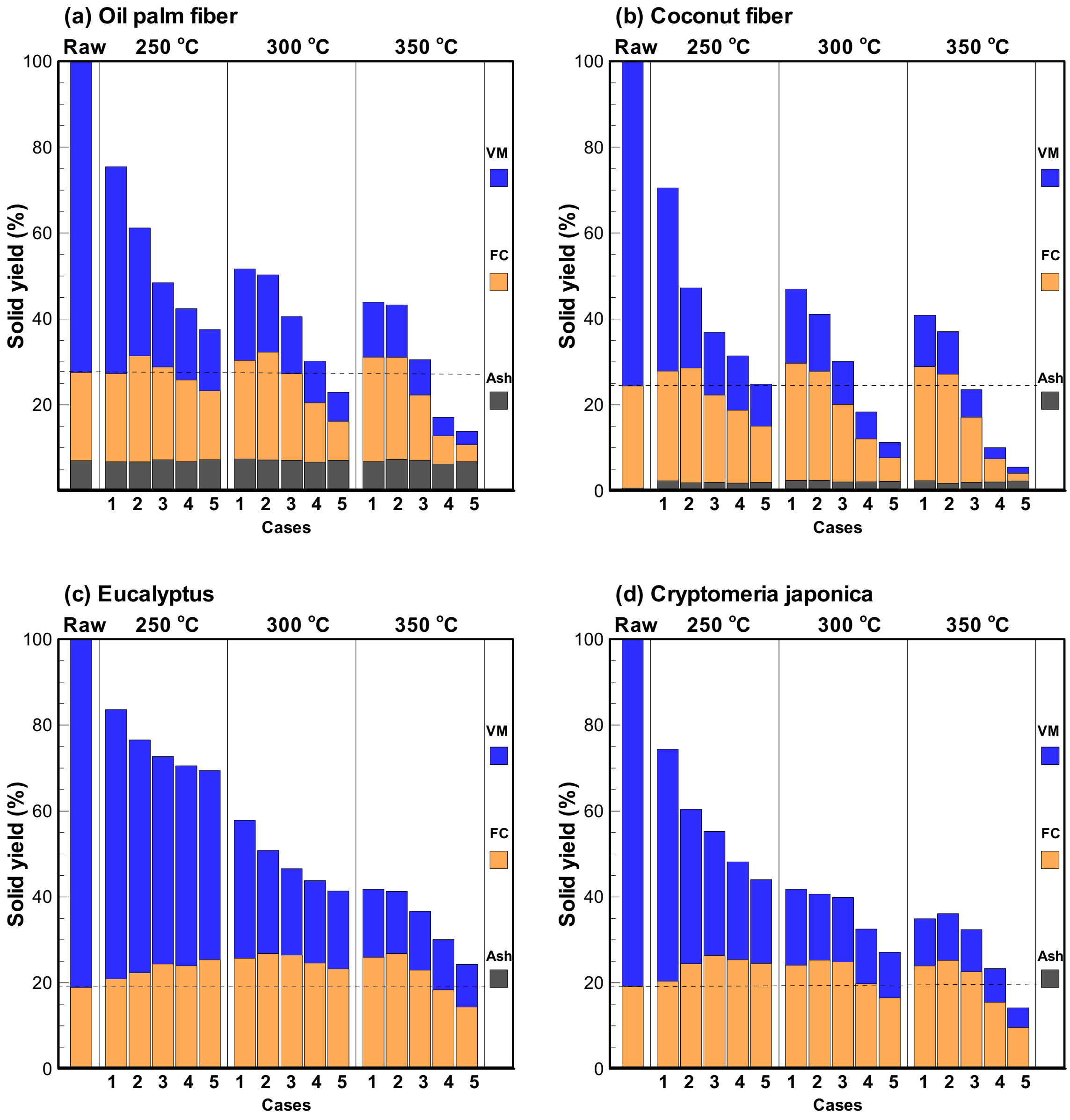

Fig. 3. The profiles of the solid yields and proximate analyses of raw and torrefied (a) OPF, (b) CF, (c) EU, and (d) CJ.

Table 2
Elemental analyses of untreated and torrefied biomass at various air superficial velocities.

Material	Temperature (°C)	Superficial velocity[a] (cm min^{-1})	Elemental analysis (wt%, db[b])			
			C	H	O[c]	N
Oil palm fiber	Untreated		51.94	4.75	40.88	2.43
	250	N_2[d]	57.52	5.57	35.49	1.42
		0.82	68.26	4.47	25.60	1.67
		4.08	67.87	2.92	26.82	2.39
		8.15	65.99	3.38	27.95	2.68
		12.23	67.48	2.29	26.98	3.25
	300	N_2	70.07	4.90	23.38	1.65
		0.82	70.63	3.31	23.44	2.62
		4.08	70.06	2.70	24.15	3.09
		8.15	68.28	2.61	25.84	3.27
		12.23	68.66	3.80	24.79	2.75
	350	N_2	76.76	3.82	17.32	2.10
		0.82	77.75	3.57	16.74	1.94
		4.08	75.89	2.50	18.78	2.83
		8.15	68.89	2.75	22.74	5.62
		12.23	67.60	1.64	23.40	7.36
Coconut fiber	Untreated		51.77	4.43	42.87	0.93
	250	N_2	60.59	5.19	33.41	0.81
		0.82	70.18	3.22	26.20	0.40
		4.08	69.57	2.06	28.00	0.37
		8.15	67.49	1.91	30.12	0.48
		12.23	69.10	1.79	28.60	0.51
	300	N_2	72.45	3.92	22.97	0.66
		0.82	73.91	2.67	23.12	0.30
		4.08	74.56	1.84	23.20	0.40
		8.15	71.58	1.66	26.08	0.68
		12.23	69.97	1.53	27.39	1.11
	350	N_2	76.55	3.37	19.46	0.62
		0.82	79.42	2.57	17.75	0.26
		4.08	78.54	1.92	19.07	0.47
		8.15	72.98	1.86	24.36	0.80
		12.23	63.69	1.43	33.84	1.04
Eucalyptus	Untreated		50.77	5.13	44.10	0.00
	250	N_2	57.96	4.96	36.87	0.21
		0.82	58.67	4.82	36.51	0.00
		4.08	59.06	4.36	36.58	0.00
		8.15	60.67	4.26	35.07	0.00
		12.23	58.91	4.13	36.96	0.00
	300	N_2	68.42	4.18	27.40	0.00
		0.82	72.36	3.73	23.91	0.00
		4.08	72.74	2.74	24.52	0.00
		8.15	71.48	2.19	26.33	0.00
		12.23	71.91	2.20	25.89	0.00
	350	N_2	75.22	3.61	21.17	0.00
		0.82	74.88	2.98	22.02	0.12
		4.08	72.29	2.15	25.56	0.00
		8.15	75.03	1.20	23.77	0.00
		12.23	69.99	1.22	28.75	0.04
Cryptomeria japonica	Untreated		51.73	5.30	42.80	0.17
	250	N_2	58.16	5.19	36.65	0.00
		0.82	65.40	4.79	29.46	0.35
		4.08	65.56	3.81	30.63	0.00
		8.15	69.06	3.15	27.79	0.00
		12.23	68.39	2.35	29.26	0.00
	300	N_2	73.30	4.35	22.35	0.00
		0.82	75.21	3.95	20.75	0.09
		4.08	73.33	3.10	23.57	0.00
		8.15	74.09	2.25	23.66	0.00
		12.23	71.15	2.00	26.85	0.00
	350	N_2	77.03	3.64	19.33	0.00
		0.82	78.72	3.24	18.04	0.00
		4.08	77.09	2.38	20.53	0.00
		8.15	76.49	1.76	21.75	0.00
		12.23	75.55	1.73	22.61	0.11

[a] Air superficial velocities of 0.82, 4.08, 8.15 and 12.23 cm min^{-1} correspond to the air flow rates of 100, 500, 1000 and 1500 mL min^{-1}, respectively.
[b] Dry basis.
[c] By difference.
[d] N_2 superficial velocity is 8.15 mL min^{-1} (N_2 flow rate = 1000 mL min^{-1}).

of 100, 500, 1000 and 1500 mL min^{-1}. Meanwhile, three different torrefaction temperatures of 250, 300, and 350 °C are considered.

The contents of volatile matter (VM), fixed carbon (FC), and ash in raw and torrefied materials as well as the solid yield are

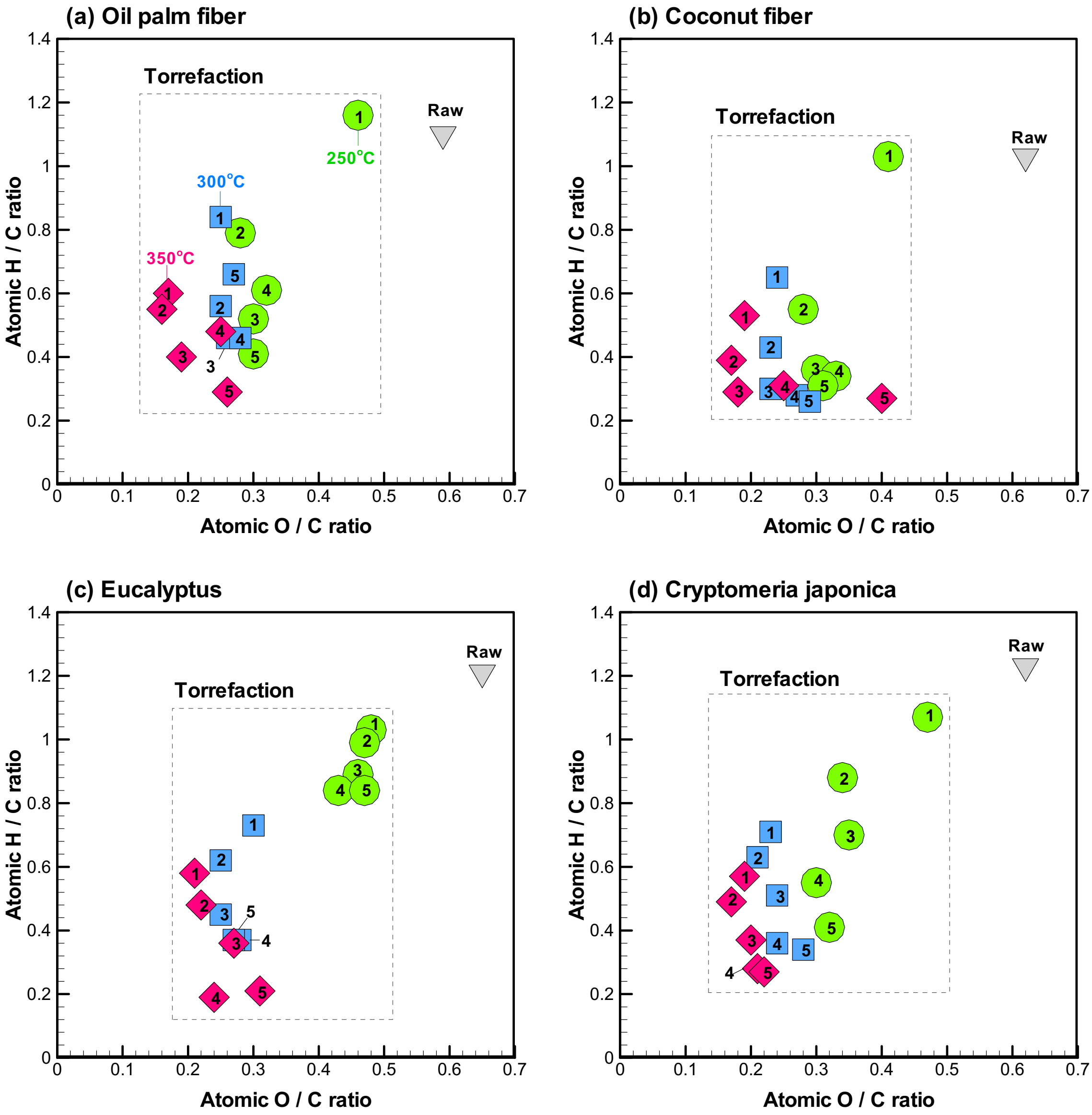

Fig. 4. The van Kelvelen diagrams (atomic H/C ratio versus atomic O/C ratio) of raw and torrefied (a) OPF, (b) CF, (c) EU, and (d) CJ.

demonstrated in Fig. 3. After undergoing non-oxidative torrefaction (Case 1), an increase in torrefaction temperature significantly lowers the VM content, whereas the FC content in the four materials is only slightly affected, mainly at air superficial velocities of 0.82 and 4.08 cm min^{-1}. This clearly elucidates the dominant mechanism of devolatilization in the course of biomass torrefaction in an inert atmosphere. With regard to the oxidative torrefaction (Cases 2–5), more oxidative reaction is involved when the air superficial velocity increases. Seeing that OPF and CF have higher surface areas (needle-shape) compared to EU and CJ, the fixed carbon in the two samples is consumed in Cases 3–5 at temperatures of 300 and 350 °C (Fig. 3a and b). This indicates that the surface oxidation plays an important role in the consumption of fixed carbon. In examining the profiles of EU and CJ (Fig. 3c and d), the devolatilization process is also enhanced when the temperature or air superficial velocity increases. However, their fixed carbon contents are relatively insensitive to the temperature and air superficial velocity, except for CJ at 350 °C in Cases 4 and 5. This can be explained by the small surface areas of the two samples due to the block-shape. In fact, the FC contents in the torrefied materials are even higher than those in the raw materials in some cases, presumably due to the carbonization of volatile matter while it is liberated from biomass (Chen et al., 2011d).

As far as the solid yield is concerned, the values for the four samples torrefied in N_2 (Case 1) at 250 °C are higher than 70 wt%, and they are less than 50 wt% when they are torrefied at 350 °C. For OPF and CF with oxidative torrefaction at 250 °C, when the air superficial velocity increases, there is a significant decay in solid yield and the devolatilization process corresponds to the lowered solid yield. With the torrefaction temperatures of 300 and 350 °C, the FC contents of OPF and CF are also abated at the superficial velocities no less than 4.08 cm min^{-1}. Their solid yields are thus fairly low (<30 wt%). According to the profiles, OPF and CF should be torrefied at temperatures no larger than 250 °C and air superficial velocities no larger than 0.82 cm min^{-1} in that at least around 50 wt% of solid residue can be retained. Considering the torrefaction of EU and CJ, increasing air superficial velocity also lessens the solid yield; however, its impact is not as pronounced as that on OPF and CF. Within the investigated ranges of temperature and air superficial velocity, Fig. 3c and d suggest that the influence

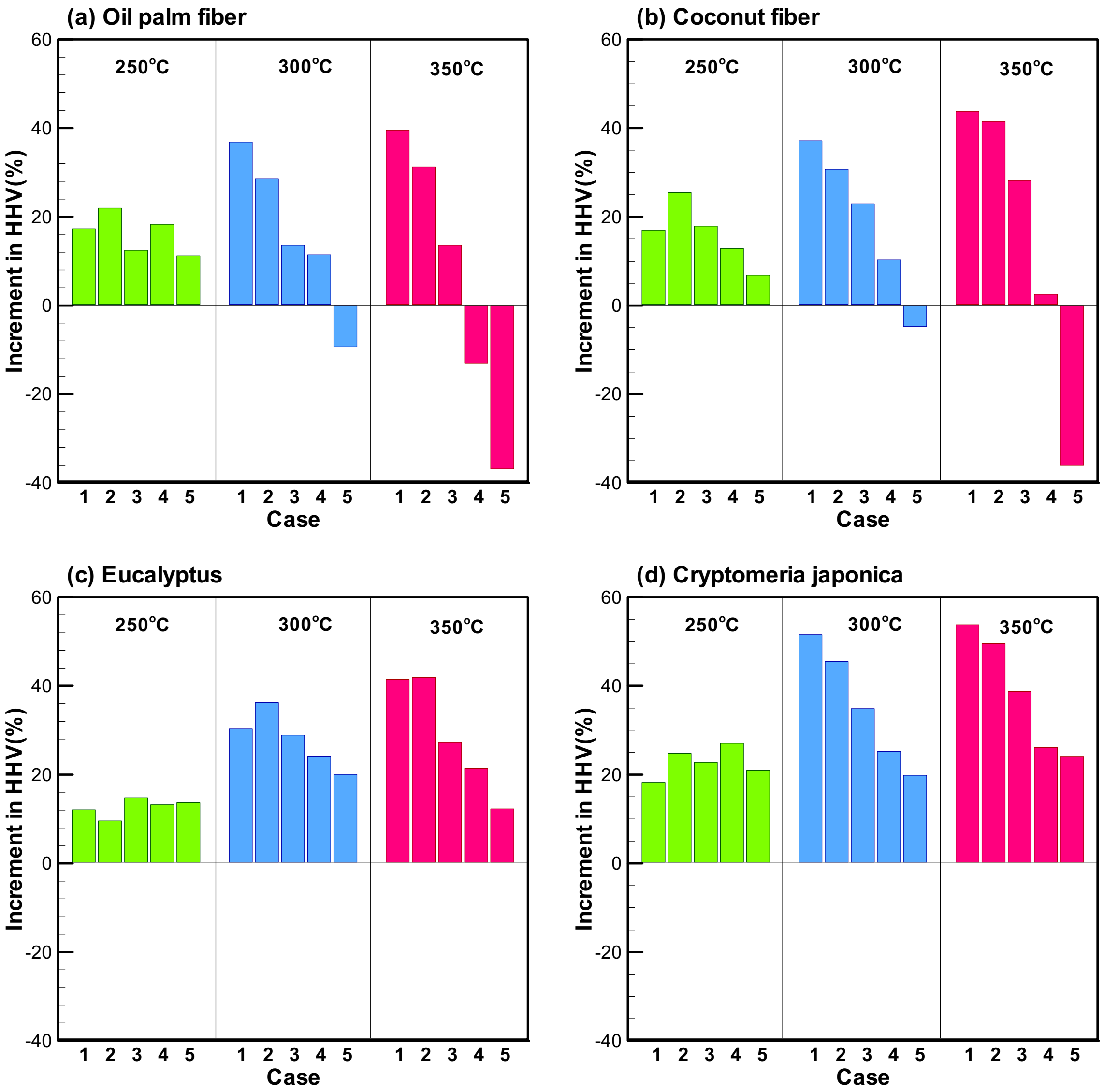

Fig. 5. The profiles of the HHV increment of torrefied (a) OPF, (b) CF, (c) EU, and (d) CJ.

of the former on the solid yield prevails over the latter. As a whole, EU torrefied at 250 °C is able to give a high solid yield, regardless of the air superficial velocity. CJ can be torrefied at 250 °C with air superficial velocities no larger than 4.08 cm min^{-1} in that over 55 wt% of solid yield is obtained.

3.3. Elemental analysis

It has been known that the relative contents of elemental oxygen and hydrogen in biomass are reduced when it is torrefied, whereas the relative content of elemental carbon rises (Chew and Doshi, 2011; Uemura et al., 2011; Chen et al., 2012a). The detailed values of the elemental analyses of the four materials are given in Table 2 and the profiles of atomic H/C ratio versus atomic O/C ratio (van Kelvelen diagram) are displayed in Fig. 4. The digits embedded in the symbols represent the case number. Similar to conventional torrefaction, oxidative torrefaction has a trend to decrease both the atomic H/C and O/C ratios. Overall, increasing torrefaction temperature tends to reduce the two ratios. However, it is noteworthy that varying air superficial velocity has an influence on the atomic H/C ratio, whereas the atomic O/C ratio is relatively insensitive to the air superficial velocity.

3.4. HHV and energy yield

The increment in the HHV of biomass from torrefaction is plotted in Fig. 5. For the two fibrous biomass materials (OPF and CF), their HHVs can be improved if the temperature and the air superficial velocity are not larger than 300 °C and 8.15 cm min^{-1}, respectively. The negative increment in HHV at high temperatures and air superficial velocity is owing to the substantial decrease in FC (Fig. 3a and b). Besides, the relative content of ash is increased in the torrefied biomass. Alternatively, the HHVs of the two ligneous biomass materials (EU and CJ) can always be enhanced, regardless of the temperature and air superficial velocity. At the torrefaction temperature of 250 °C, the correlation between the increment of HHV and the air superficial velocity is not pronounced, as a consequence of relatively weak oxidation. In the study of Rousset et al. (2012b), they illustrated that the temperature had an important effect on the HHV of EU under the oxidative torrefaction at 240 and 280 °C, but the oxygen concentration (oxidative atmosphere) didn't significantly affect the HHV of torrefied EU. Basically, the results shown in Fig. 5c are similar to their observations. With the torrefaction temperatures of 300 and 350 °C, the increment in HHV tends to decrease with increasing air superficial velocity. This can be explained by the obvious oxidative reaction.

Based on the solid yield and the HHV increment, the profiles of the energy yields of the four materials are provided in Fig. 6. The energy yield is defined by the energy ratio between the torrefied biomass and its raw biomass, which is equivalent to the multiplication of solid yield and (1+ the increment in HHV). Regarding the torrefaction of OPF and CF under the conditions of temperature greater than or equal to 300 °C and air superficial velocity greater than or equal to 4.08 cm min^{-1}, there is a drastic drop in energy (Fig. 6a and b). With the torrefaction temperature of 350 °C and air superficial velocities no less than 8.15 cm min^{-1}, the energy yield is even lower than 15%. This arises from the double impacts of oxidative torrefaction in lessening solid yield (Fig. 3a and b) and HHV increment (Fig. 5a and b). It is thus summarized that the torrefaction of fibrous biomass at high temperatures and air superficial velocities should be avoided. For EU and CJ, they can be torrefied in both inert and oxidative atmospheres if the temperature is at 250 °C in that over 45% of energy yield is retained (Fig. 6c and d).

Rousset et al. (2012b) and Uemura et al. (2013) pointed out that the solid yield of biomass with oxidative torrefaction decreased with increasing oxygen concentration. In contrast, an increase in air superficial velocity leading to the decrease in solid yield is exhibited in the present study. To proceed farther into an analysis of the role played by oxygen superficial velocity on the solid yield, HHV increment, energy yield, and energy-mass co-benefit index (EMCI), their equations of linear regression at 300 °C are tabulated in Table 3 where the value of oxygen superficial velocity is the multiplication of 0.21 and air superficial velocity because the oxygen flow rate is 21% of the air flow rate. A high value of EMCI of torrefied biomass stands for the biomass featured by a higher energy density and a lower volume (Lu et al., 2012b). As a whole, the coefficient of determination (R^2) is between 0.81 and 0.99, implying that the four physical scales are correlated well, except for the increment in the HHV of EU ($R^2 = 0.776$). The negative slopes of the regression lines clearly suggest that a higher oxygen

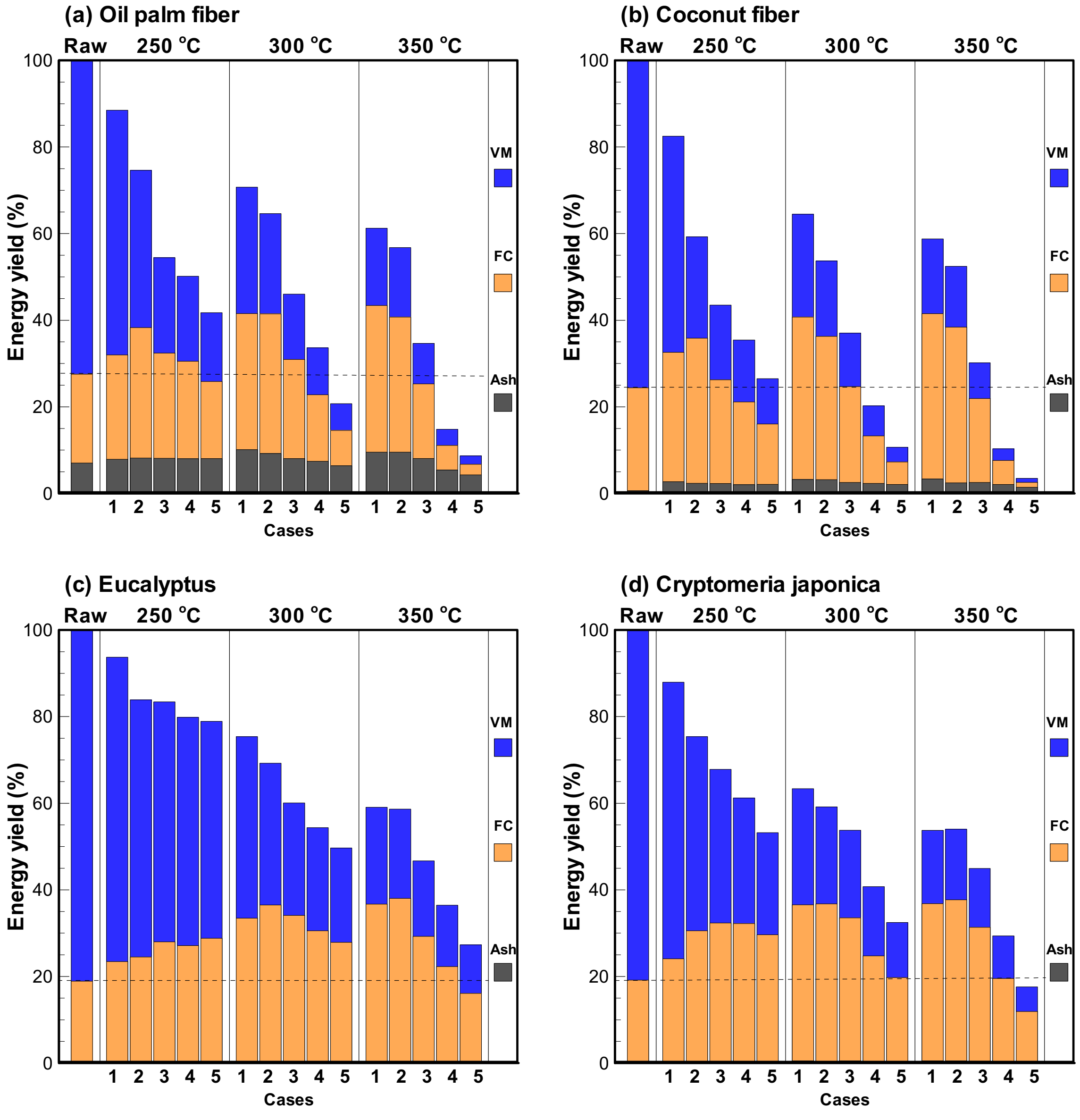

Fig. 6. The profiles of the energy yields and proximate analyses of raw and torrefied (a) OPF, (b) CF, (c) EU, and (d) CJ.

Table 3
The equations of linear regression of solid yield, HHV increment, energy yield, and EMCI of torrefied biomass versus O_2 superficial velocity at 300 °C.

Property	Biomass	Linear regression	R^2
Solid yield[a]	Oil palm fiber	$y = -11.72x + 51.72$	0.990
	Coconut fiber	$y = -13.75x + 44.14$	0.975
	Eucalyptus	$y = -5.62x + 54.83$	0.810
	Cryptomeria japonica	$y = -5.80x + 42.72$	0.958
Increment in HHV[b]	Oil palm fiber	$y = -15.41x + 30.47$	0.892
	Coconut fiber	$y = -15.93x + 37.32$	0.976
	Eucalyptus	$y = -5.49x + 34.93$	0.776
	Cryptomeria japonica	$y = -12.25x + 47.97$	0.942
Energy yield[c]	Oil palm fiber	$y = -19.02x + 66.20$	0.966
	Coconut fiber	$y = -20.52x + 58.83$	0.960
	Eucalyptus	$y = -9.76x + 73.65$	0.881
	Cryptomeria japonica	$y = -12.06x + 62.62$	0.986
EMCI[d]	Oil palm fiber	$y = -19.02x + 66.20$	0.842
	Coconut fiber	$y = -20.52x + 58.83$	0.915
	Eucalyptus	$y = -9.76x + 73.65$	0.881
	Cryptomeria japonica	$y = -12.06x + 62.62$	0.954

[a] $x = O_2$ superficial velocity (cm min^{-1}); y = solid yield (%).
[b] $x = O_2$ superficial velocity (cm min^{-1}); y = increment in HHV (%).
[c] $x = O_2$ superficial velocity (cm min^{-1}); y = energy yield (%).
[d] $x = O_2$ superficial velocity (cm min^{-1}); y = EMCI.

superficial velocity linearly decreases the values of the four physical scales. The value of the slope also means the sensitivity of a physical scale to oxygen superficial velocity. Accordingly, Table 3 indicates that the solid yields, HHV increments, and energy yields of OPF and CF are more sensitive to oxygen superficial velocity compared to EU and CJ. The impact of increasing oxygen superficial velocity on EU is the lowest among the four materials in that the regression line of EU has the largest slope.

In summary, though using air as the carrier gas for biomass torrefaction is able to reduce the operating cost, the oxidative reaction along the biomass surface has a negative impact of on the performance of biomass torrefaction, especially for fibrous biomass. Therefore, how to obtain a balance between operating cost and torrefaction performance by means of oxidative torrefaction deserves further study in the future.

4. Conclusions

The reaction characteristics of biomass torrefaction in inert and oxidative atmospheres at various superficial velocities have been investigated. The results suggest that the reaction is controlled by heat and mass transfer in biomass when it is torrefied in nitrogen. For biomass torrefied in air, surface oxidation is the dominant mechanism in pretreating biomass. The surface oxidation intensifies the internal heat and mass transfer when the temperature and superficial velocity are raised. This results in a significant drop in solid and energy yields. At a fixed temperature, there is an upper limit for surface oxidation when even more air is supplied.

Acknowledgement

The authors gratefully acknowledge the financial support of China Steel Corporation for this study.

References

Chen, W.H., Kuo, P.C., 2011. Isothermal torrefaction kinetics of hemicellulose, cellulose, lignin and xylan using thermogravimetric analysis. Energy 36, 6451–6460.

Chen, W.H., Tu, Y.J., Sheng, H.K., 2010. Impact of dilute acid pretreatment on the structure of bagasse for producing bioethanol. Int. J. Energy Res. 34, 265–274.

Chen, W.H., Hsu, H.C., Lu, K.M., Lee, W.J., Lin, T.C., 2011a. Thermal pretreatment of wood (Lauan) block by torrefaction and its influence on the properties of the biomass. Energy 36, 3012–3021.

Chen, W.H., Cheng, W.Y., Lu, K.M., Huan, Y.P., 2011b. An evaluation on improvement of pulverized biomass property for solid fuel through torrefaction. Appl. Energy 88, 3636–3644.

Chen, W.H., Tu, Y.J., Sheen, H.K., 2011c. Disruption of sugarcane bagasse lignocellulosic structure by means of dilute sulfuric acid pretreatment with microwave-assisted heating. Appl. Energy 88, 2726–2734.

Chen, Q., Zhou, J.S., Liu, B.J., Mei, Q.F., Luo, Z.Y., 2011d. Influence of torrefaction pretreatment on biomass gasification technology. Chin. Sci. Bull. 56, 1449–1456.

Chen, W.H., Lu, K.M., Tsai, C.M., 2012a. An experimental analysis on property and structure variations of agricultural wastes undergoing torrefaction. Appl. Energy 100, 318–325.

Chen, W.H., Ye, S.C., Sheen, H.K., 2012b. Hydrolysis characteristics of sugarcane bagasse pretreated by dilute acid solution in a microwave irradiation environment. Appl. Energy 93, 237–244.

Chew, J.J., Doshi, V., 2011. Recent advances in biomass pretreatment-torrefaction fundamentals and technology. Renew. Sust. Energy Rev. 15, 4212–4222.

Chiang, K.Y., Chien, K.L., Lu, C.H., 2012. Characterization and comparison of biomass produced from various sources: suggestions for selection of pretreatment technologies in biomass-to-energy. Appl. Energy 100, 164–171.

Chouchene, A., Jeguirim, M., Khiari, B., Zagrouba, F., Trouvé, G., 2010. Thermal degradation of olive solid waste: influence of particle size and oxygen concentration. Resour. Conserv. Recycl. 54, 271–277.

Duncan, A., Pollard, A., Fellouah, H., 2013. Torrefied, spherical biomass pellets through the use of experimental design. Appl. Energy 101, 237–243.

Fang, M.X., Shen, D.K., Li, Y.X., Yu, C.J., Luo, Z.Y., Cen, K.F., 2006. Kinetic study on pyrolysis and combustion of wood under different oxygen concentrations by using TG–FTIR analysis. J. Anal. Appl. Pyrol. 77, 22–27.

Ghetti, P., Ricca, L., Angelini, L., 1996. Thermal analysis of biomass and corresponding pyrolysis products. Fuel 75, 565–573.

Huang, Y.F., Chen, W.R., Chiueh, P.T., Kuan, W.H., Lo, S.L., 2012. Microwave torrefaction of rice straw and pennisetum. Bioresour. Technol. 123, 1–7.

Li, J., Brzdekiewicz, A., Yang, W., Blasiak, W., 2012a. Co-firing based on biomass torrefaction in a pulverized coal boiler with aim of 100% fuel switching. Appl. Energy 99, 344–354.

Li, H., Liu, X., Legros, R., Bi, X.T., Lim, C.J., Sokhansanj, S., 2012b. Pelletization of torrefied sawdust and properties of torrefied pellets. Appl. Energy 93, 680–685.

Li, H., Liu, X., Legros, R., Bi, X.T., Lim, C.J., Sokhansanj, S., 2012c. Torrefaction of sawdust in a fluidized bed reactor. Bioresour. Technol. 103, 453–458.

Lu, K.M., Lee, W.J., Chen, W.H., Lin, T.C., 2012a. Thermogravimetric analysis and kinetics of co-pyrolysis of raw/torrefied wood and coal blends. Appl. Energy 100, 318–325.

Lu, K.M., Lee, W.J., Chen, W.H., Liu, S.H., Lin, T.C., 2012b. Torrefaction and low temperature carbonization of oil palm fiber and eucalyptus in nitrogen and air atmospheres. Bioresour. Technol. 123, 98–105.

Lynam, J.G., Coronella, C.J., Yan, W., Reza, M.T., Vásquez, V.R., 2011. Acetic acid and lithium chloride effects on hydrothermal carbonization of lignocellulosic biomass. Bioresour. Technol. 102, 6192–6199.

Munir, S., Daood, S.S., Nimmo, W., Cunliffe, A.M., Gibbs, B.M., 2009. Thermal analysis and devolatilization kinetics of cotton stalk, sugar cane bagasse and shea meal under nitrogen and air atmospheres. Bioresour. Technol. 100, 1413–1418.

Peng, J.H., Bi, H.T., Sokhansanj, S., Lim, J.C., 2012. A study of particle size effect on biomass torrefaction and densification. Energy Fuels 26, 3826–3839.

Prins, M.J., Ptasinski, K.J., Janssen, F.J.J.G., 2006. Torrefaction of wood: Part 1. Weight loss kinetics. J. Anal. Appl. Pyrol. 77, 28–34.

Rousset, P., Petithuguenin, T., Rodrigues, T., Azevedo, A.C., 2012a. The fluidization behaviour of torrefied biomass in a cold model. Fuel 102, 256–263.

Rousset, P., Macedo, L., Commandré, J.M., Moreira, A., 2012b. Biomass torrefaction under different oxygen concentrations and its effect on the composition of the solid by-product. J. Anal. Appl. Pyrol. 96, 86–91.

Saravanakumar, A., Haridasan, T.M., Reed, T.B., Bai, R.K., 2007. Experimental investigation and modelling study of long stick wood gasification in a top lit updraft fixed bed gasifier. Fuel 86, 2846–2856.

Tapasvi, D., Khalil, R., Skreiberg, Ø., Tran, K.Q., Grønli, M., 2012. Torrefaction of norwegian birch and spruce: an experimental study using macro-TGA. Energy Fuels 26, 5232–5240.

Tran, K.Q., Luo, X., Seisenbaeva, G., Jirjis, R., 2013. Stump torrefaction for bioenergy application. Appl. Energy, http://dx.doi.org/10.1016/j.apenergy.2012.12.053.

Uemura, Y., Omar, W.N., Tsutsui, T., Yusup, S.B., 2011. Torrefaction of oil palm wastes. Fuel 90, 2585–2591.

Uemura, Y., Omar, W., Othman, N.A., Yusup, S., Tsutsui, T., 2013. Torrefaction of oil palm EFB in the presence of oxygen. Fuel 103, 156–160.

Wang, C., Peng, J., Li, H., Bi, X.T., Legros, R., Lim, C.J., Sokhansanj, S., 2013. Oxidative torrefaction of biomass residues and densification of torrefied sawdust to pellets. Bioresour. Technol. 127, 318–325.

Wannapeera, J., Worasuwannarak, N., 2012. Upgrading of woody biomass by torrefaction under pressure. J. Anal. Appl. Pyrol. 96, 173–180.

Wongsiriamnuay, T., Tippayawong, N., 2010. Thermogravimetric analysis of giant sensitive plants under air atmosphere. Bioresour. Technol. 101, 9314–9320.

Yan, W., Acharjee, T.C., Coronella, C.J., Vásquez, V.R., 2009. Thermal pretreatment of lignocellulosic biomass. Environ. Prog. Sustain. Energy 28, 435–439.